Available online at www.sciencedirect.com
ScienceDirect
Polymer 48 (2007) 6145–6151
polymer
www.elsevier.com/locate/polymer

Analysis of inner structure in high-strength biodegradable fibers by X-ray microtomography using synchrotron radiation

Toshihisa Tanaka [a,d], Kentaro Uesugi [b], Akihisa Takeuchi [b], Yoshio Suzuki [b], Tadahisa Iwata [c,d,*]

[a] *Faculty of Textile Science and Technology, Shinshu University, 3-15-1 Tokida, Ueda-shi, Nagano 386-8567, Japan*
[b] *Japan Synchrotron Radiation Research Institute (JASRI), 1-1-1 Kouto, Sayo-cho, Sayo-gun, Hyogo 679-5198, Japan*
[c] *Department of Biomaterial Sciences, Graduate School of Agricultural and Life Sciences, The University of Tokyo, 1-1-1 Yayoi, Bunkyo-ku, Tokyo 113-8657, Japan*
[d] *Ecomolecular Science Research II, RIKEN Institute, 2-1 Hirosawa, Wako-shi, Saitama 351-0198, Japan*

Received 12 December 2006; received in revised form 16 July 2007; accepted 26 July 2007
Available online 2 August 2007

Abstract

The observation of the inner structure of materials without pretreatment or damage is a very useful analytical method in the field of materials science as well as in medicine and biology. We have carried out a three-dimensional (3D) analysis of biodegradable polyester bacterial-poly[(*R*)-3-hydroxybutyrate-*co*-(*R*)-3-hydroxyvalerate] (P(3HB-*co*-3HV)) fibers with high tensile strength (1.07 GPa) using X-ray microtomography with synchrotron radiation. The inner structure of the fibers was visualized at a spatial resolution of 1 μm. There are many fine voids for one-step-drawn P(3HB-*co*-3HV) fibers after isothermal crystallization from the result of X-ray microtomography. This revealed that the clear streak reflection along the equator in small-angle X-ray scattering is caused by these fine voids. The recalculated tensile strength of one-step-drawn P(3HB-*co*-3HV) fibers after isothermal crystallization is suggested to be 2.02 GPa, taking the cross-section area with 52.7% (polymer region) into consideration. These fine voids in fibers seemed to be generated by the volume changes due to the contraction of polymer chains during isothermal crystallization.

Keywords: Poly[(*R*)-3-hydroxybutyrate-*co*-(*R*)-3-hydroxyvalerate]; X-ray microtomography; High-strength biodegradable fiber

1. Introduction

Fibers of poly[(*R*)-3-hydroxybutyrate] (P(3HB)) and its copolymers have attracted much attention as biodegradable polyester fibers for use as fishing lines and surgical sutures [1]. P(3HB) and its copolymers are synthesized by a variety of bacteria from renewable carbon sources and degraded to water and carbon dioxide by bacteria in soil, seawater, and river water [1–3]. Recently, we succeeded in producing high-strength poly-[(*R*)-3-hydroxybutyrate-*co*-(*R*)-3-hydroxyvalerate] (P(3HB-*co*-3HV)) fibers with a tensile strength at break of 1.1 GPa. These were processed by one-step-drawing after isothermal crystallization in ice water near the glass transition temperature to prevent rapid crystallization and to enable the formation of small crystal nuclei [4].

Fig. 1 shows scanning electron micrographs and the two-dimensional small-angle X-ray scattering (SAXS) patterns of one-step-drawn P(3HB-*co*-3HV) fibers after isothermal crystallization in ice water or without isothermal crystallization [4]. While the two sets of fibers have similar morphologies (Fig. 1(a) and (a′)), their SAXS patterns are completely different. The SAXS pattern of a one-step-drawn fiber without isothermal crystallization (Fig. 1(b)) yields clear two-spot reflections along the meridian, suggesting that there are lamellar crystals of systematic long period along the fiber axis. On the other hand, it is difficult to detect any spot reflection along the meridian in the SAXS patterns of one-step-drawn fibers after isothermal crystallization (Fig. 1(b′)). Streak scattering can

* Corresponding author. Department of Biomaterial Sciences, Graduate School of Agricultural and Life Sciences, The University of Tokyo, 1-1-1 Yayoi, Bunkyo-ku, Tokyo 113-8657, Japan. Tel.: +81 3 5841 7888; fax: +81 3 5841 1304.
E-mail address: atiwata@mail.ecc.u-tokyo.ac.jp (T. Iwata).

0032-3861/$ - see front matter © 2007 Elsevier Ltd. All rights reserved.
doi:10.1016/j.polymer.2007.07.063

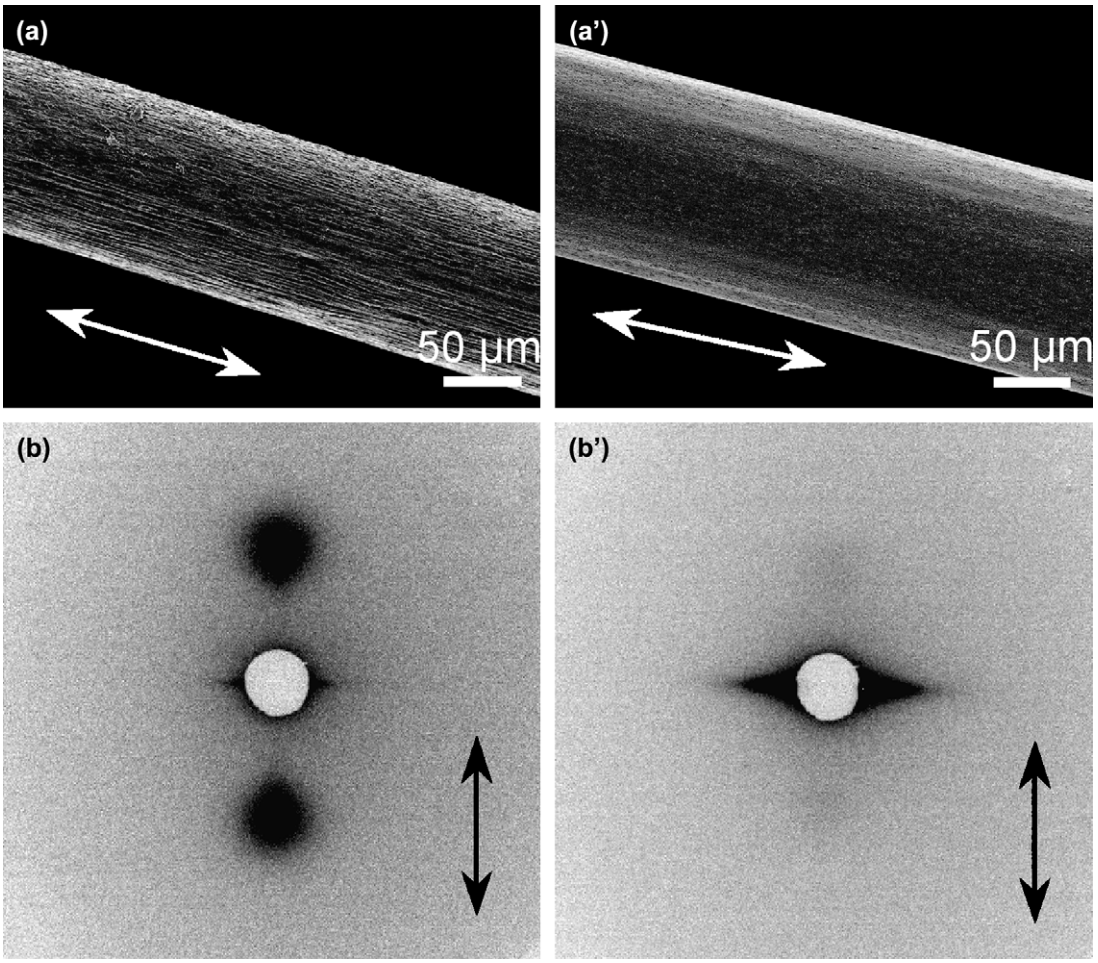

Fig. 1. SEM and SAXS patterns of 10 times one-step-drawn P(3HB-*co*-3HV) fibers: (a, b) without isothermal crystallization, and (a′, b′) after isothermal crystallization [4]. The arrows indicate the drawing direction.

be clearly seen along the equator perpendicular to the drawing direction. In the past, this streak scattering along the equator was noted in highly oriented fibers and was considered to be due to voids in the fibers or the interface of the fiber. However, until now, there has been no direct evidence for relation between the streak scattering and the presence of voids. Therefore, we made an attempt to analyze inner structure of P(3HB-*co*-3HV) fibers by using X-ray microtomography method as the interesting approach to understand the inner structure of polymer materials without damage and necessity of pretreatment.

In addition to its traditional use in medical diagnosis, X-ray tomography has recently begun to be employed for evaluating materials and for non-destructive testing. X-ray tomography is a useful technique for analyzing the inner structure of materials [5], since transmitted images can be obtained and used to reconstruct cross-sectional images. Furthermore, three-dimensional (3D) images can be obtained by superimposing the cross-sectional images. Generally, the data obtained from X-ray measurements give the spatial distribution of the X-ray linear absorption coefficient. This is a function of the density of material and of the mass absorption coefficient determined by irradiated X-ray energy. In other words, the transmitted images of a material depend on factors such as X-ray intensity, elementary composition, density, or quantity of material. Differences between transmitted quantities (the so-called X-ray light absorption coefficient) reveal information on the inner structure of a material. However, when X-rays pass through materials beam, hardening occurs together with changes of spectra and of the transmitted intensity of the X-rays, even if the material is uniform. It is therefore necessary to employ monochromatic X-rays of sufficiently high intensity in order to prevent beam hardening and to perform quantitative analyses.

Synchrotron radiation is very effective in producing high X-ray intensity. Since spatial resolution increases with X-ray intensity, synchrotron radiation of high intensity yields measurements at high resolution. X-ray measurements using synchrotron radiation have proved useful for characterizing the dynamic behavior of polymer morphology, crystal transitions, structures during deformation and thermal treatment, and for drawing [6–8]. Recently, phase contrast tomography using synchrotron radiation of 10 μm has been employed for 3D analyses using differences of the refractive distribution coefficient in polymer/polymer blends such as the polystyrene/poly(methyl methacrylate) system [9]. For instance of

investigation on fibers, X-ray tomography was also used to visualize floc concentration for the pulp and nylon fiber suspension [10], and silicon carbide (SiC) fiber bundles in SiC matrix/Nicalon fiber composites [11]. The highest spatial resolution of X-ray tomography achieved in three-dimensions was about 1 μm, using Fresnel Zone Plate optics [12]. Therefore, X-ray microtomography measurements using synchrotron radiation are considered to be a very useful method for characterizing the inner structure of fibers. In this study, we set out to analyze the inner structure of one-step-drawn P(3HB-*co*-3HV) fibers by X-ray microtomography at the SPring-8 synchrotron radiation facility.

2. Experimental section

2.1. Sample preparation

Poly[(*R*)-3-hydroxybutyrate-*co*-(*R*)-3-hydroxyvalerate] (P(3-HB-*co*-3HV)) was supplied by Monsanto Co., Japan. The M_w and polydispersity of P(3HB-*co*-3HV) were 1.0×10^6 and 2.8, respectively. The composition of the 3HV unit determined by ^{1}H nuclear magnetic resonance (^{1}H NMR) in $CDCl_3$ was 7.7%.

Melt-spinning of P(3HB-*co*-3HV) was carried out using a laboratory-size extruder (IMC-1149, Imoto Machinery, Japan). P(3HB-*co*-3HV) was extruded at 170 °C, which is higher than the melting temperature. The molten polymer was taken up by rolling and directly quenched in an ice water bath to obtain amorphous fibers. The drawing procedures were as described previously [4]. These involved (a) one-step-drawing using a stretching machine at room temperature without isothermal crystallization, and (b) one-step-drawing using a stretching machine at room temperature after isothermal crystallization for a constant period in an ice water bath at near the glass transition temperature. The effect of isothermal crystallization is to prevent rapid crystallization and initiate the growth of small crystal nuclei. All fibers were annealed at 60 °C in a hot oven under constant tension for 30 min to increase their crystallinity.

2.2. Analytical procedures

The high resolution X-ray microtomography system was developed using beamline BL47XU with a wavelength of 0.15497 nm at 8 keV in the SPring-8 synchrotron radiation facility in Japan. The system consists of high precision stages using a light source, a double crystal monochromator, and a high spatial resolution X-ray image detector (CCD-based image detector (Hamamatsu Photonics, Japan K. K., C4880-41S)) with exposure times of 300 ms (Fig. 2). Samples were fixed on a rotation rod, which was placed in the X-ray beam. For 3D analysis of P(3HB-*co*-3HV) fibers measurements were made perpendicular to the fiber axis, and samples were rotated in steps of 0.2° angles. The effective pixel size was 0.2 μm, and the format of the CCD camera was 2000×1312 in 2×2 binning mode. The number of bits per pixel was 12. Convolution back projection, as the mathematically equivalent method with filtered back projection, which

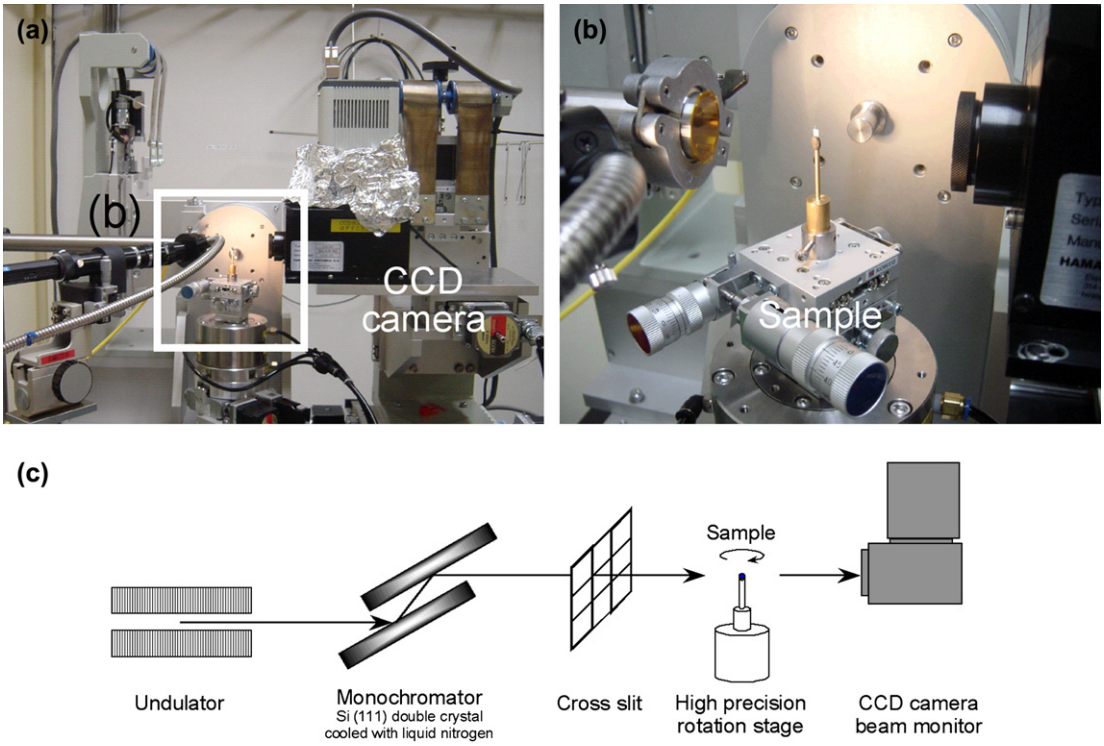

Fig. 2. (a, b) Photographs of the X-ray microtomography measurement system using beamline BL47XU with a wavelength of 0.15497 nm at 8 keV at the SPring-8 synchrotron radiation facility in Japan. (b) Magnified image of the boxed area in (a). (c) Illustration of the measuring system. The exposure time and the rotation angle were 300 ms and 0.2°, respectively.

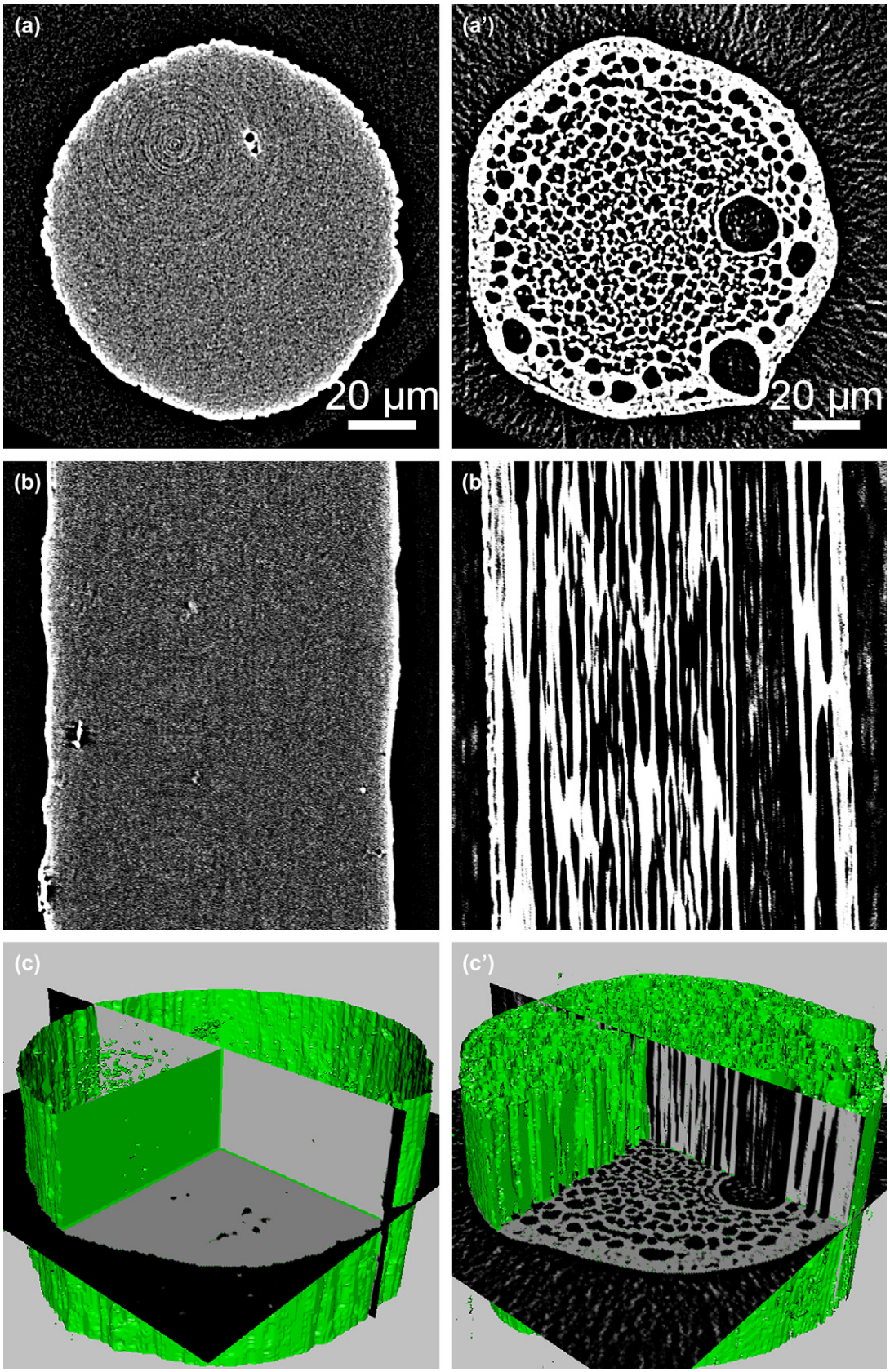

Fig. 3. Reconstructed images of 10 times one-step-drawn P(3HB-*co*-3HV) fibers: (a, a′) cross-sections perpendicular to the drawing direction, (b, b′) cross-sections parallel to the drawing direction, and (c, c′) stereoscopic models. Left and right rows represent one-step-drawn fibers without and after isothermal crystallization, respectively.

was programmed by Dr. K. Uesugi, was used for tomographic reconstruction. Three-dimensional reconstruction software (Studio PON, Forge version 2.0) was used to superimpose the X-ray tomography cross-sectional images, and image analysis software (Media Cybernetics, Inc., Image Pro Plus version 4.0) was used to calculate cross-sectional areas and sizes of voids.

Scanning electron micrograph (SEM) images of the surface of samples were taken with a JEOL JSM-6330F microscope after the samples were coated with gold using a SC-701 quick coater (SANYU DENSHI, Japan). The two-dimensional (2D) SAXS experiments were carried out using beamline BL45XU with a wavelength of 0.09 nm at the SPring-8 synchrotron radiation facility. A monofilament was set up perpendicular to the X-ray beam and parallel to the detector, and diffraction patterns were recorded with a charge-coupled-device (CCD) camera (C7300-10-12NR, Hamamatsu Photonics) with exposure times of 76–1058 ms. The pixel size of the CCD camera was 125×125 μm, and there were 12 bits per pixel. The camera length for SAXS measurements was 2200 mm.

3. Results and discussion

One-step-drawn P(3HB-*co*-3HV) fibers were placed on a rod perpendicular to the fiber axis in order to rotate and expose the fibers to the X-ray beam as shown in Fig. 2. The transmitted images obtained were restructured to cross-sectional images and stereoscopic models were constructed by superimposing these images. Fig. 3 shows the X-ray microtomography cross-sectional images and stereoscopic model for one-step-drawn P(3HB-*co*-3HV) fibers (100–120 μm diameter) with and without isothermal crystallization. The cross-sectional images perpendicular and parallel to the drawing direction of the one-step-drawn fiber without isothermal crystallization are uniform throughout the fiber (Fig. 3(a–c)). However, after isothermal crystallization, the one-step-drawn fiber has many fine voids of cohesive elliptic shape in the drawing direction (Fig. 3(a′–c′)). Thus, we have visualized the 3D inner structure of high-strength fibers. The results show that the streak scattering in the SAXS pattern shown in Fig. 1(b′) is due to the presence of many fine voids throughout the fiber.

The size and distribution of voids in the one-step-drawn P(3HB-*co*-3HV) fibers after isothermal crystallization were analyzed by image analysis software. The distribution of void diameters in cross-sections perpendicular to the drawing direction is shown in Fig. 4. Most void diameters were 1.0–1.6 μm and the average was 2.3 ± 1.5 μm.

Cross-sectional area versus load stress is an important parameter for evaluating the tensile strength of materials. To assess the mechanical properties of a uniaxial structure with many fine voids such as the one-step-drawn P(3HB-*co*-3HV) fiber after isothermal crystallization (Fig. 3(c′)) one needs to know its true cross-sectional area. We therefore derived the cross-sectional areas of the oriented fiber from the cross-sectional images perpendicular to the drawing direction using image analytical software. The calculated tensile strengths

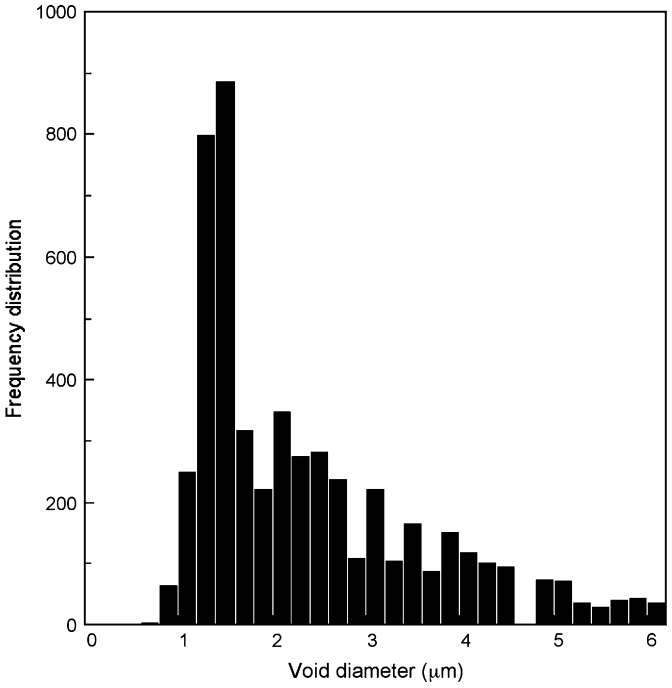

Fig. 4. Distribution of void diameters perpendicular to the drawing direction derived from the cross-sectional images (Fig. 3(a′)) by image analysis software in a 10 times one-step-drawn P(3HB-*co*-3HV) fiber after isothermal crystallization.

derived from the recalculated cross-sections for one-step-drawn P(3HB-*co*-3HV) fibers with and without isothermal crystallization are summarized in Table 1. The recalculated cross-sectional area determined by X-ray microtomography analysis was the same as the apparent cross-sectional area for the one-step-drawn P(3HB-*co*-3HV) fiber without isothermal crystallization and agreed with previous results [4]. However, the recalculated cross-sectional area of the one-step-drawn P(3HB-*co*-3HV) fiber after isothermal crystallization was 52.7% of the apparent cross-sectional area. Therefore, the tensile strength determined by recalculation of the cross-sectional area for the latter fiber is considered to be 2020 MPa. This calculated value indicates that the physical properties of P(3HB-*co*-3HV) fibers are highly suitable for use as biodegradable materials. The fact that it has been impossible to obtain high-strength fibers of the theoretically obtainable strength until now is probably due to the presence of the fine voids in the highly oriented fibers.

To understand the formation mechanism of voids, we performed the 3D observation of non-drawn fibers by using X-ray microtomography measurement. Fig. 5 shows the X-ray cross-section images for non-drawn P(3HB-*co*-3HV) fibers without and after isothermal crystallization. There is no fine void except the large voids in non-drawn fiber without isothermal crystallization (Fig. 5(a and b)). These large voids are suggested to form by the entry of air or water during fiber preparation such as melt-spinning. However, there are fine globular voids in addition to large voids in non-drawn fibers after isothermal crystallization as shown in the circles of Fig. 5(a′). The cross-section along the line of I′ in Fig. 5(a′)

Table 1
Apparent and calculated cross-sectional areas, and tensile strengths of 10 times one-step-drawn P(3HB-*co*-3HV) fibers with and without isothermal crystallization near the glass transition temperature

Isothermal crystallization time (h)	Apparent cross-section		Tensile strength (MPa)[a]	Calculated cross-section		Calculated tensile strength (MPa)[b]
	Area (μm^2)	Ratio (%)		Area (μm^2)	Ratio (%)	
0	1.21×10^4	100	90	1.21×10^4	99.9	90
24	1.29×10^4	100	1065	0.68×10^4	52.7	2020

[a] Obtained from the apparent cross-sectional areas in Ref. [4].
[b] Recalculated from measured cross-sectional areas (1065/0.527 = 2020 MPa).

displays the three-dimensional distribution of fine voids throughout the fiber (Fig. 5(b′)). The diameter of non-drawn fiber after isothermal crystallization indicated no remarkable decrease due to isothermal crystallization. The generation of many fine voids in one-step-drawn P(3HB-*co*-3HV) fibers after isothermal crystallization probably results from partially contraction of the polymer chains and the entry of water during isothermal crystallization before drawing, or from thermal shrinkage of the polymer chains and outflow of water during annealing after drawing. The morphology of the 3D structure with many fine cohesive elongated voids in one-step-drawn fibers, and tomographic image in non-drawn fibers after isothermal crystallization supports the latter explanation. In other words, fine voids develop by the partial shrinkage of polymer chains during crystallization process at glass transition temperature with no significant change in diameter of fibers. Therefore, a mechanism for generating many fine voids in one-step-drawn P(3HB-*co*-3HV) fibers after isothermal crystallization is proposed as follows; the large voids are formed by the entry of air or water when melt-spinning, on

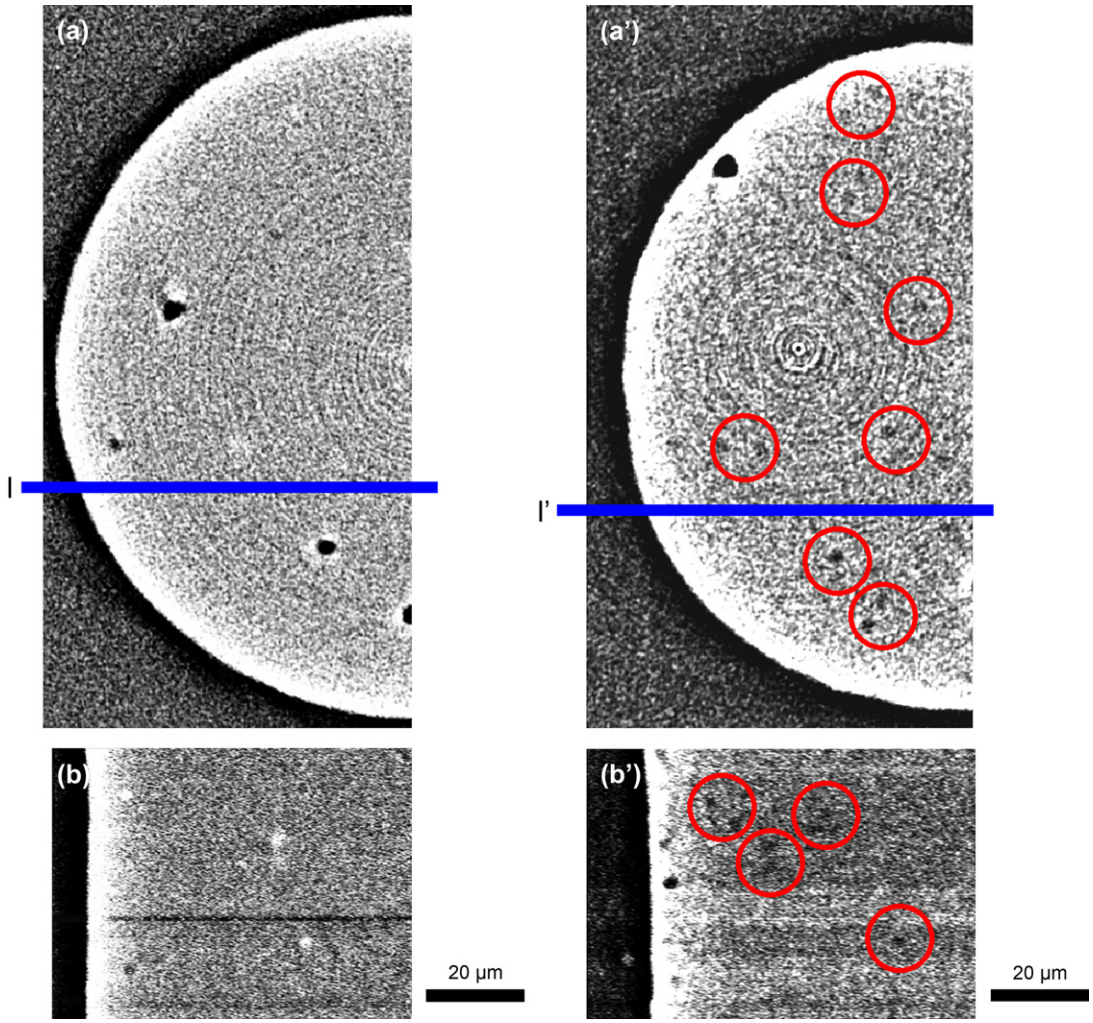

Fig. 5. Reconstructed images of non-drawn P(3HB-*co*-3HV) fibers: (a, a′) cross-sections perpendicular to the drawing direction, (b, b′) cross-sections parallel to the drawing direction at each position along the line of I, I′, respectively. Left and right rows represent non-drawn fibers without and after isothermal crystallization, respectively. The circles indicate fine voids generated by the contraction of polymer chains during isothermal crystallization.

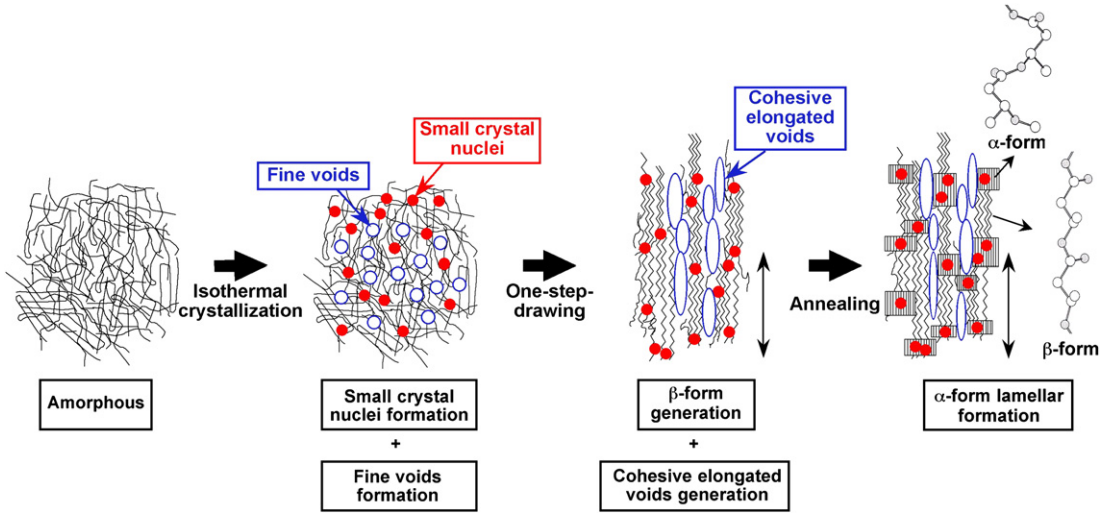

Fig. 6. Schematic display for generating fine voids and two crystal conformations in high-strength P(3HB-*co*-3HV) fibers by one-step-drawing after isothermal crystallization. The vertical arrows indicate the drawing direction. This figure was obtained by the addition to Fig. 8 in Ref. [4].

the other hand, the fine voids are generated by the contraction of polymer chains during isothermal crystallization before drawing (see Fig. 6).

X-ray microtomographic measurement of polymer fibers with voids is a unique produce for the evaluation and analysis of their inner structure without causing damage and excluding the need for pretreatment. Furthermore, this method for biodegradable polymers should prove helpful for investigating mechanisms of enzymatic degradation as well as for detecting defects such as cracking and crazing.

4. Conclusions

We have applied X-ray microtomography with synchrotron radiation to the 3D observation of high tensile strength fibers of bacterial-P(3HB-*co*-3HV). The inner structure for uniaxial oriented fibers was analyzed by X-ray microtomography measurement at a spatial resolution of 1 μm. There are many fine voids with diameter of 1.0–1.6 μm from the result of X-ray microtomography cross-section images for one-step-drawn P(3HB-*co*-3HV) fibers after isothermal crystallization. This revealed that the clear streak reflection along the equator in small-angle X-ray scattering is caused by these fine voids. The one-step-drawn P(3HB-*co*-3HV) fibers after isothermal crystallization is suggested to have a potential with high tensile strength of 2.0 GPa from recalculation of cross-section area perpendicular to the drawing direction. The fine voids are supposed to generate by the contraction of polymer chains during isothermal crystallization.

Acknowledgments

This work was supported by a Grant-in-Aid for Scientific Research (B) from the Ministry of Education, Culture, Sports, Science and Technology (MEXT) of Japan (No. 19350075) (to T. Iwata). The synchrotron radiation experiments were performed at the SPring-8 with the approval of the Japan Synchrotron Radiation Research Institute (JASRI) (Proposals No. 2005A0307 and No. 2005B0039).

References

[1] Lenz RW, Marchessault RH. Biomacromolecules 2005;6:1–8.
[2] Holmes PA. In: Bassett DC, editor. Developments in crystalline polymers, vol. 2. London: Elsevier Applied Science; 1988. p. 1–65.
[3] Doi Y. Microbial polyesters. Weinheim: VCH Publishers; 1990.
[4] Tanaka T, Fujita M, Takeuchi A, Suzuki Y, Uesugi K, Ito K, et al. Macromolecules 2006;39:2940.
[5] Bonse U, Busch F. Prog Biophys Mol Biol 1996;65:133.
[6] Riekel C, Garcia Gutierrez MC, Gourrier A, Roth S. Anal Bioanal Chem 2003;376:594.
[7] Chu B, Hsiao BS. Chem Rev 2001;101:1727.
[8] Iwata T, Aoyagi Y, Fujita M, Yamane H, Doi Y, Suzuki Y, et al. Macromol Rapid Commun 2004;25:1100.
[9] Momose A, Fujii A, Kadowaki H, Jinnai H. Macromolecules 2005;38:7197.
[10] Ringner J, Rasmuson A. Nordic Pulp Paper Res J 2000;15:319.
[11] Kinney JH, Nichols MC. Annu Rev Mater Sci 1992;22:121.
[12] Suzuki Y, Takeuchi A, Takano H, Ohigashi T, Takenaka T. Jpn J Appl Phys 2001;40:1508.